

Parameter estimation with cluster states

Matthias Rosenkranz* and Dieter Jaksch†

Clarendon Laboratory, University of Oxford, Parks Road, Oxford OX1 3PU, United Kingdom and
Keble College, Parks Road, Oxford OX1 3PG, United Kingdom

(Dated: October 27, 2018)

We propose a scheme for parameter estimation with cluster states. We find that phase estimation with cluster states under a many-body Hamiltonian and separable measurements leads to a precision at the Heisenberg limit. As noise models we study the dephasing, depolarizing, and pure damping channels. Decoherence reduces the sensitivity but our scheme remains superior over several reference schemes with states such as maximally entangled states and product states. For small cluster states and fixed evolution times it remains at the Heisenberg limit for approximately 2 times as many qubits than alternative schemes.

PACS numbers: 03.65.Ta, 03.67.-a, 06.20.Dk

I. INTRODUCTION

The precise determination of system parameters by measurements is the basis of many applications in physics and beyond. Quantum mechanics offers a way to enhance measurement sensitivity by lowering the theoretically achievable limits. It is a long-standing goal in the quantum parameter estimation field to find feasible ways to reach this so-called Heisenberg limit. We call the number of physical systems used to measure the parameter (e.g., the number of atoms or photons) the *resource size*. In the Heisenberg limit, the measurement precision scales with the inverse resource size. In contrast, the classical shot-noise limit scales only with the inverse square root of the resource size. Examples of emerging quantum technology applications based on this enhancement are improved frequency standards [1], the construction of quantum clocks and their synchronization [2], the detection of weak forces [3], or the improved resolution and signal-to-noise ratio in image reconstruction [4, 5]. A straightforward proposal to achieve the Heisenberg limit in principle by using maximally entangled states faces the problem that these states are also more sensitive to background noise and hence decoherence. In general this leads to a diminishing or complete cancellation of the overall improvement of these schemes [6]. In this paper, we present a scheme based on cluster states, which are a class of entangled states. They are well known in the context of quantum computation [7] but, to our knowledge, their relevance in parameter estimation theory has not yet been investigated. Cluster states prove very robust against many sources of noise [8, 9]. We combine this robustness with a scheme capable of estimating a phase parameter of the system evolution.

The main results of our proposal can be summarized as (i) cluster states attain the Heisenberg limit for a setup with a three-body Hamiltonian and no decoherence. In atomic systems, cluster states have been implemented with neutral atoms in an optical lattice [10]. Also many other proposals on how to create cluster states exist, for example, with ions [11], in

cavities [12, 13], in charge and flux qubits [14], and with the help of a linear quantum register [15, 16]. Proposals for implementing Hamiltonians of the form considered in this paper have been put forward for neutral atoms in optical lattices [17] and cold polar molecules [18]. It should be noted that recent works have shown that the Heisenberg limit is not the ultimate lower bound in quantum metrology, but that it can be beaten by implementing Hamiltonians with symmetric k -body interactions [19–21]. (ii) All required measurements are of a simple tensor product form involving only single Pauli measurements. (iii) Decoherence leads to a decrease in measurement precision but our scheme remains superior to various reference schemes. In implementations with cold atoms, the main contribution to decoherence is dephasing noise, which we study in detail in this paper. Furthermore, we consider depolarization and damping noise, which represent smaller contributions to the overall decoherence in typical realizations. Our first reference system is given by a standard quantum metrology scheme with different Hamiltonian and initial states than the cluster state scheme. This will show that our scheme improves on the precision of these standard schemes. The second reference system consists of the Hamiltonian of the cluster state scheme but with different initial states. This will demonstrate that one can only expect this improvement for a suitable combination of Hamiltonian and initial state.

Cluster states have been implemented in purely optical setups using polarization and momentum entanglement of photons currently for up to six qubits [22–26]. The measurements required for our scheme can also be realized optically. We are not aware of proposals to implement the Hamiltonian of our proposed scheme in an optical system and developing such a proposal is beyond the scope of the present paper. Decoherence in the optical case is mainly caused by photon loss, which is not discussed here [27].

This paper is organized as follows. After the introduction of parameter estimation theory and cluster states, we discuss in Sec. II how cluster states can be employed in parameter estimation schemes. It turns out that, in principle, it is possible to achieve the Heisenberg limit with this cluster state scheme. We also define our reference systems. In Sec. III, we show how dephasing noise influences the precision of the measurements. We discuss an analytical model of the cluster state measurement scheme and present our main numerical re-

*Electronic address: m.rosenkranz@physics.ox.ac.uk

†URL: <http://www.physics.ox.ac.uk/qubit/>

sults. These results are compared with an alternative estimation scheme and we find an overall improvement of precision even under noise. Two further noise channels, namely the depolarizing and damping channels, are considered in Sec. IV, with qualitatively similar results. In Sec. V, we consider a further reference system subjected to all three noise channels. The scaling with the number of resources when we include noise is discussed in Sec. VI. There we show that our scheme offers advantages for small resource sizes. We conclude the paper in Sec. VII and explicitly derive an analytical solution for our model with resource size $N = 2$ in an appendix.

II. PARAMETER ESTIMATION SCHEMES

In this section, we introduce the basics of parameter estimation theory and cluster states. Subsequently, we combine the two and introduce a scheme of parameter estimation with cluster states. Finally, we present the reference systems we will be using throughout the paper.

A. Parameter estimation theory

We consider a system with Hamiltonian $H_\chi = \chi H_0$ and density operator $\rho(t)$ which evolves according to the von Neumann equation ($\hbar = 1$)

$$\frac{d\rho}{dt}(t) = i[\rho(t), H_\chi]. \quad (1)$$

Parameter estimation aims to determine the value of the parameter χ by means of suitable measurements on many copies of the system. Repeated measurements of an operator O result in ν data points o_i . It is then possible to extract an estimate for χ from this data by means of an estimator $\chi_{\text{est}}(o_1, \dots, o_\nu)$. The uncertainty of the estimation is expressed as

$$\delta\chi = \left\langle \left(\frac{\chi_{\text{est}}}{|d\langle\chi_{\text{est}}\rangle/d\chi|} - \chi \right)^2 \right\rangle^{1/2}. \quad (2)$$

The denominator cancels superfluous ‘‘units’’ introduced by the estimator. If we assume an unbiased estimator, i.e., $\langle\chi_{\text{est}}\rangle = \chi$, then the uncertainty, Eq. (2), reduces to the deviation of the estimator, which is a familiar measure of precision.

If we let $\rho(t)$ be a pure state, then it can be shown that the uncertainty $\delta\chi$ is bounded by [19, 28–30]

$$\delta\chi \geq \frac{1}{2\sqrt{\nu}t\Delta H_0}. \quad (3)$$

ΔH_0 is the standard deviation of H_0 , i.e., $\Delta H_0 = \sqrt{\langle H_0^2 \rangle - \langle H_0 \rangle^2}$. The bound Eq. (3) is also called quantum Cramér-Rao bound. There are two routes available to minimizing the uncertainty. The factor $\sqrt{\nu}$ in the denominator of Eq. (3) is the well-known statistical improvement with the number of independent runs ν . In general, this $1/\sqrt{\nu}$ scaling is attained in the limit of many runs of the experiment [30].

Here we are not interested in this trivial improvement. The second and more interesting way is to maximize ΔH_0 .

Consider N replicas of a physical system evolving according to the Hamiltonian $H_\chi = \chi H_0$ with

$$H_0 = \sum_{j=1}^N h_0^{(j)}, \quad (4)$$

where $h_0^{(j)}$ is the Hamiltonian of the j th replica. We assume that each replica undergoes the same evolution so that each $h_0^{(j)}$ is of the same form. The maximal deviation of the composite Hamiltonian H_0 is then attained by evolving the maximally entangled state

$$|\psi\rangle = \frac{1}{\sqrt{2}} \left(|\lambda_{\min}\rangle^{\otimes N} + |\lambda_{\max}\rangle^{\otimes N} \right),$$

where $|\lambda_{\min}\rangle$ and $|\lambda_{\max}\rangle$ are the eigenvectors of $h_0^{(j)}$ with the smallest and largest eigenvalues λ_{\min} and λ_{\max} , respectively. This state yields $\Delta H_0 = N(\lambda_{\max} - \lambda_{\min})/2$, and we see that the generalized uncertainty, Eq. (3), is given by

$$\delta\chi \geq \frac{1}{\sqrt{\nu}tN(\lambda_{\max} - \lambda_{\min})}.$$

Such a scaling with the inverse of the resource size, here N , is called Heisenberg scaling and the corresponding precision measurement is said to attain the Heisenberg limit. Note that this limit can be reached by using only separable measurements on each constituent [29]. In contrast, if we use uncorrelated states initially, the scaling is proportional to $1/\sqrt{N}$, which is known as the standard quantum limit. Quantum metrology offers an improvement of $1/\sqrt{N}$ over classical schemes for Hamiltonians of the form in Eq. (4). However, in realistic setups the von Neumann equation is rarely exactly realized owing to the presence of environmental noise. Intuitively one would expect noise to deteriorate the precision. In fact, Huelga *et al.* [6] and others [31, 32] found that decoherence rapidly destroys the improvement gained in a straightforward implementation with maximally entangled states. They also point out the existence of partially entangled states which do improve the precision even under noise. This paper aims to improve on this result by introducing the more robust cluster states into quantum metrology.

B. Cluster states

Cluster states are a particular type of many-body entangled states [8, 33]. Their mathematical description is based on the notion of graphs. A graph G consists of a finite nonempty set V of N vertices together with a finite set E of m unordered pairs of distinct vertices from V [34]. Elements of E are also called edges since they join two vertices. Based on this notion we define the family of operators

$$K^{(i)} = \sigma_x^{(i)} \prod_{j \in N(i)} \sigma_z^{(j)}, \quad i \in V,$$

where $N(i)$ denotes the set of vertices sharing an edge with the i th vertex, and a Pauli operator $\sigma_{x,y,z}^{(i)}$ acts only on the i th vertex. A graph state $|+G\rangle$ is defined as the unique eigenstate with $K^{(i)}|+G\rangle = |+G\rangle$ for all operators $K^{(i)}$. The group \mathcal{S}_G generated under multiplication by the set $\{K^{(i)} | i \in V\}$ is called the stabilizer of the graph state. It is instructive to identify the vertices with a two-level physical system, which we will henceforth denote as qubit. With this notation, an equivalent way of describing graph states is given by first initialising every qubit in the superposition $(1/\sqrt{2})(|0\rangle + |1\rangle)$ and then applying a controlled phase gate between each pair of qubits connected by an edge in the graph [33].

For simplicity, in this paper, we reduce the class of all valid graphs to linear graphs, which results in one-dimensional (1D) cluster states. Here, all vertices are connected to exactly two neighbors, which are pairwise distinct (except the first and last vertex, which are connected to one neighbor each). In physical terms one could imagine a string of atoms, for example, each interacting with its next neighbors only. This leads to the family of stabilizers

$$K^{(i)} = \sigma_z^{(i-1)} \sigma_x^{(i)} \sigma_z^{(i+1)} \quad (5)$$

for $1 \leq i \leq N$, where N is the number of vertices (or, equivalently, qubits). We use the convention that $\sigma_z^{(0)} = \sigma_z^{(N+1)} = 1$. Cluster states are known to be remarkably stable against a range of sources of noise [8, 9, 35, 36]. This stability can be traced to the fact that local decoherence on an individual qubit in the composite state only affects the small set of its neighbors. For cluster states, the number of neighbors does not depend on the total number of qubits but is a constant of the underlying graph. In this work we will exploit this feature to achieve a higher measurement precision even under the influence of noise.

C. Parameter estimation scheme with cluster states

We have seen in Sec. II A that superpositions of states with maximally separated eigenvalues of H_0 together with appropriate measurements are sufficient to reach the Heisenberg limit. In Sec. II B we have introduced 1D cluster states as eigenstates of a family of correlators $K^{(i)}$. In analogy to the simple case of independent one-body Hamiltonians for a system of N qubits, we sum the correlators of all vertices and interpret this sum as a Hamiltonian

$$H_{II} = \frac{\chi}{2} \sum_{j=1}^N K^{(j)} = \frac{\chi}{2} \sum_{j=1}^N \sigma_z^{(j-1)} \sigma_x^{(j)} \sigma_z^{(j+1)}. \quad (6)$$

Here, χ is the parameter we would like to estimate and j counts the qubits. In an atomic optical lattice implementation of this Hamiltonian [18], the parameter χ would sensitively depend on the atomic scattering properties. In a purely optical setup, measuring χ could reveal the values of high-order terms in the susceptibility of the medium with high precision. Let $|+N\rangle$ be a 1D cluster state of N qubits so that $K^{(i)}|+N\rangle = |+N\rangle$ for all i . It is straightforward to

see that the state $|-N\rangle := \prod_{j=1}^N \sigma_z^{(j)} |+N\rangle$ is an eigenstate with $K^{(i)}|-N\rangle = -|-N\rangle$ for all i . To prove this note that $\sigma_z^{(j)}$ commutes with $K^{(i)}$ for $i \neq j$ but anticommutes for $i = j$ [37]. This is analogous to the eigenstates $|0\rangle$ and $|1\rangle$ of the single particle Hamiltonians $h_0^{(i)} = \sigma_z^{(i)}$ in conventional quantum metrology schemes [6]. We use a superposition of eigenstates, cluster states, of the underlying Hamiltonian as a resource, namely,

$$|\psi_c\rangle = \frac{1}{\sqrt{2}}(|+N\rangle + |-N\rangle). \quad (7)$$

Here and in the following, an index c on a quantity denotes that this quantity belongs to the cluster state setup. Subsequently, the system evolves under H_{II} for a time t before it is measured. The time evolution leaves the system in the state

$$|\psi_c\rangle_t = \frac{1}{\sqrt{2}} \left(e^{-iN\chi t/2} |+N\rangle + e^{iN\chi t/2} |-N\rangle \right).$$

As measurement operator we employ

$$M_c = \prod_{j=1}^N \sigma_z^{(j)}. \quad (8)$$

The expectation value and deviation of M_c are

$$\langle M_c \rangle = \cos(N\chi t), \quad (9)$$

$$\Delta M_c = |\sin(N\chi t)|. \quad (10)$$

We now consider ν independent runs of the experiment. In order to calculate the uncertainty, Eq. (2), inherent in this setup, we define an estimator implicitly via

$$\frac{1}{\nu} \sum_{j=1}^{\nu} M_c^{(j)} =: \cos(N\chi_{\text{est}} t), \quad (11)$$

where $M_c^{(j)}$ is the measurement operator for the j th independent run. This estimator is unbiased, which can be seen by expanding the right-hand side of Eq. (11) around the actual coupling χ up to first order and taking the expectation value combined with Eq. (9). This reduces the uncertainty, Eq. (2), to the deviation

$$\delta\chi_c = \Delta\chi_{\text{est}} = \frac{\Delta M_c}{\sqrt{\nu} N t |\sin(N\chi t)|} = \frac{1}{\sqrt{\nu} t N}.$$

Hence, our setup achieves the Heisenberg scaling $1/N$ in the decoherence-free case. In this sense, the measurement operator M_c we chose is optimal for this setup. The factor $1/\sqrt{\nu}$ originates from statistical averaging over ν measurements. The $1/\sqrt{N}$ improvement over the shot-noise limit is the result of the N -fold increase of the frequency in the expectation value of M_c .

As with all phase measurement schemes, the periodicity of the expectation value, Eq. (9), and estimator, Eq. (11), result in an ambiguity when globally determining the value of χ without prior knowledge. However, we expect our setup to be a good candidate for local phase determination when the initial value of the parameter is known with a good accuracy [38].

D. Reference systems

In the following sections, we compare the attainable precision of our cluster state setup with different reference systems. The cluster state setup is defined by the Hamiltonian $H_\chi = H_{II}$, Eq. (6), the initial state $|\psi_c\rangle$, Eq. (7), and the measurement M_c , Eq. (8). This setup is always kept invariant in these comparisons.

1. Reference system (I)

The first reference system is the standard system used in parameter estimation. It is defined by the Hamiltonian

$$H_I = \frac{\chi}{2} \sum_{j=1}^N \sigma_z^{(j)}.$$

We then use two different initial states, which evolve under this Hamiltonian, and corresponding measurement operators. These are given by

$$|\psi_m\rangle = \frac{1}{\sqrt{2}} \left(|0\rangle^{\otimes N} + |1\rangle^{\otimes N} \right), \quad M_m = \prod_{j=1}^N \sigma_x^{(j)}, \quad (12)$$

$$|\psi_u\rangle = \left(\frac{1}{\sqrt{2}} (|0\rangle + |1\rangle) \right)^{\otimes N}, \quad M_u = \sum_{j=1}^N \sigma_x^{(j)}. \quad (13)$$

The indices m and u indicate quantities corresponding to maximally entangled and uncorrelated states, respectively. The measurement operators M_m and M_u are optimal for attaining the lowest deviation in the decoherence-free case with the respective initial state [29]. If we include dephasing noise in this setup, we recover the result in [6] that maximally entangled states lead to the same minimal deviation $\delta\chi$ as uncorrelated states. The origin for this behavior is the N -fold increase in the decoherence rate for maximally entangled state compared to uncorrelated states.

2. Reference system (II)

The Hamiltonian for our second reference system is given by H_{II} , Eq. (6). As in reference system (I) we use maximally entangled and uncorrelated states as initial states for the parameter estimation. This means that we can compare cluster state parameter estimation with parameter estimation with different initial states under the same Hamiltonian H_{II} . Also the measurement operators for the respective states are the same as before. Hence, reference system (II) is defined by Hamiltonian H_{II} , Eq. (6), together with Eqs. (12) and (13) as initial states and measurements.

III. PARAMETER ESTIMATION UNDER DEPHASING NOISE

Physical systems are often exposed to various sources of noise. In this section, we focus on individual dephasing of the qubits. Dephasing is modeled by replacing the unitary evolution Eq. (1) with the master equation

$$\frac{d\rho}{dt}(t) = i[\rho(t), H_\chi] + \frac{\gamma}{2} \sum_{j=1}^N \left[\sigma_z^{(j)} \rho(t) \sigma_z^{(j)} - \rho(t) \right]. \quad (14)$$

In this paper, we choose the Hamiltonians H_I or H_{II} for H_χ depending on the reference system we study. The parameter γ denotes the strength of the dephasing. To achieve the Cramér-Rao bound it is necessary to repeat the single measurements many times. As in [6], we assume a total run time T of the whole experiment with the duration t of each individual realization. This results in the total number of experiments $\nu = T/t$.

A. Analytical solution for $N = 2$

In this section we discuss an analytical solution of the cluster state estimation problem with the master equation (14) for the case $N = 2$. In the Appendix we present the derivation of this explicit solution. For higher N our direct approach would also yield analytical solutions, however, the complexity of the calculation rapidly becomes intractable. For $N = 2$, the expectation value and deviation of M_c are given by

$$\langle M_c \rangle(t) = e^{-\gamma t} \left(\cos(\Omega t) + \frac{\gamma}{\Omega} \sin(\Omega t) \right), \quad (15)$$

$$\delta\chi_c(t) = \frac{e^{\gamma t} \sqrt{1 - e^{-2\gamma t} \left(\cos(\Omega t) + \frac{\gamma}{\Omega} \sin(\Omega t) \right)^2}}{\sqrt{T} t \frac{4\chi}{\Omega} \left| \frac{\gamma}{\Omega} \cos(\Omega t) - \left(1 + \frac{\gamma}{\Omega^2 t} \right) \sin(\Omega t) \right|}, \quad (16)$$

where $\Omega = \sqrt{4\chi^2 - \gamma^2}$. The system frequency Ω depends on the dephasing rate but we can assume that $\gamma/2\chi \ll 1$. This is justified by the fact that in parameter estimation, in general, it is desirable to have the parameter dominating over the noise. Comparing the deviation $\delta\chi_c$ to the deviation of setup (I) with maximally entangled states,

$$\delta\chi_m(t) = \frac{e^{N\gamma t} \sqrt{1 - e^{-2N\gamma t} \cos^2(N\chi t)}}{\sqrt{T} t N |\sin(N\chi t)|}, \quad (17)$$

with $N = 2$, we see that the dephasing rate is reduced by a factor of 2. Furthermore, the additional term in $\langle M_c \rangle(t)$ is of order γ/Ω , which is given by

$$\frac{\gamma}{\Omega} = \frac{\gamma}{2\chi} \left[1 + \frac{\gamma^2}{8\chi^2} + \mathcal{O} \left(\left(\frac{\gamma}{\chi} \right)^4 \right) \right].$$

Since $\gamma/2\chi \ll 1$, the additional terms in Eq. (16) are a small perturbation compared to the solution with maximally entangled states. Similarly, the frequencies in the reference system and the cluster state setup are the same to lowest order in $\gamma/2\chi$.

We calculate the minimum of $\delta\chi_c(t)$ by first finding the envelope function of $\delta\chi_c(t)$, which is given by the solution of $\cos(\Phi) + \alpha \sin(\Phi) = 0$. We assume that $\alpha := \gamma/\Omega$ and $\Phi := \Omega t$ can be varied independently. Together with the equality $\cot(x - m\pi) = \cot(x)$, where m is an integer, this yields

$$\Omega t = \cot^{-1}(-\alpha) = \frac{k\pi}{2} + \frac{\gamma}{\Omega} + \mathcal{O}\left(\left(\frac{\gamma}{\Omega}\right)^3\right), \quad k \text{ odd.} \quad (18)$$

Plugging this into Eq. (16) results in the envelope of $\delta\chi_c(t)$

$$\delta\chi_{c,\text{env}}(t) = \frac{e^{\gamma t} \Omega^2 \sqrt{t}}{2\sqrt{T}(\gamma + 4\chi^2 t)}. \quad (19)$$

In the next step, we calculate the minimum of this envelope with respect to t , which is given by

$$t_{c,\text{min}} = \frac{1}{4\gamma} \left(1 + \sqrt{1 - \frac{3\gamma^2}{\chi^2} + \frac{\gamma^4}{4\chi^4}} \right) - \frac{\gamma}{8\chi^2}.$$

Since we have $\gamma/2\chi \ll 1$, this minimal time to lowest order is given by $t_{c,\text{min}} \approx 1/2\gamma - \gamma/8\chi^2$, which is approximately 2 times the minimal time of setup (I) with maximally entangled states [6] if we further assume that $1/2\gamma \gg \gamma/8\chi^2$. Hence, in the cluster state setup the evolution times can be longer than with maximally entangled states. It turns out that the minimal deviation $\delta\chi_{c,\text{env}}(t_{c,\text{min}})$ is lower than the one for the standard scheme (I) with maximally entangled (or uncorrelated) states. If the condition, Eq. (18), is not satisfied exactly for a particular set of parameters, then the actual lobes of the deviation still lie on the envelope but the minimum of these lobes does not coincide with the minimum of the envelope making the actual minimum of the deviation slightly larger.

We are now able to calculate the relative improvement of this scheme with respect to the reference systems. The improvement is quantified by

$$\epsilon(\gamma) = 1 - \frac{\delta\chi_{c,\text{env}}(t_{c,\text{min}})}{\delta\chi_{\text{ref}}}, \quad (20)$$

where $\delta\chi_{\text{ref}}$ is the minimum of the envelope of the reference deviation. With this definition an improvement of the cluster state scheme is given by positive values of ϵ , whereas negative values indicate that the reference system performs better. For both maximally entangled and uncorrelated states in setup (I) we have $\delta\chi_{\text{ref}} = \delta\chi_{m,\text{min}} = \delta\chi_{u,\text{min}} = \sqrt{2\gamma e/NT}$. The expansion of $\epsilon(\gamma)$ in terms of the small parameter γ/χ is given by

$$\epsilon(\gamma) = \epsilon\left(\frac{\gamma}{\chi}\right) = 1 - \frac{1}{\sqrt{2}} + \frac{3}{4\sqrt{2}} \left(\frac{\gamma}{\chi}\right)^2 + \mathcal{O}\left(\left(\frac{\gamma}{\chi}\right)^4\right). \quad (21)$$

In the limit $\gamma = 0$ this series assumes an offset $1 - 1/\sqrt{2} \approx 0.293$. In contrast, in Sec. II we have seen that the cluster state setup and the conventional setup (I) yield the same result for $\gamma = 0$. This discrepancy is owing to the fact that $t_{c,\text{min}}$ diverges as $\gamma \rightarrow 0$. For nonzero γ we always find times for which Eq. (21) holds, although for small times the two deviations can lie arbitrarily close together. The position of the minimum of the deviations increases with $1/\gamma$, so as γ decreases,

the duration of the experiment quickly exceeds experimentally reasonable time scales. If we assume a fixed maximal evolution time, the improvement can diverge from the constant for values of γ smaller than 2 times the reciprocal of this evolution time.

B. Numerical results for $N > 2$

In principle, the same analytical methods outlined above could be applied to $N > 2$. Furthermore, the analytical results could be compared to an analytical solution for reference setup (II), which would lead to qualitatively similar results. For simplicity, in the following we present numerical results of the cluster state setup and reference system (I) for higher N , and explain the findings with the insight we gained from the analytical treatment of the case $N = 2$. Our numerical results for $N = 2$ agree with the analytical solution above and known analytical solutions for arbitrary N with maximally entangled and uncorrelated states so we expect a good accuracy for the case $N > 2$. Similar to the case $N = 2$ we find that the cluster state setup beats maximally entangled states in terms of lowest deviation even for $N > 2$. In our calculations we limit the integration times to an N -dependent time $t_f(N)$. This choice illustrates the effect of a finite evolution time in experiments.

The results in Fig. 1(a) show the deviations for the $N = 7$ cluster state setup compared to maximally entangled and uncorrelated states in reference setup (I). The envelopes of the deviation for maximally entangled and uncorrelated states are given by

$$\delta\chi_{m,\text{env}} = \frac{e^{N\gamma t}}{N\sqrt{Tt}}, \quad (22)$$

$$\delta\chi_{u,\text{env}} = \frac{e^{\gamma t}}{\sqrt{NTt}}, \quad (23)$$

respectively. Note that both reference systems attain the same minimum at different times. The cluster state setup, however, attains a lower minimum than both, which is indicated by the black curve entering the shaded area in Fig. 1(a). The decay rate of the cluster state setup is approximately one-half the rate of maximally entangled states, which allows for a longer evolution time per experiment just as in the $N = 2$ case.

The numerical analysis indicates that the envelope of the cluster state setup can be approximately expressed as

$$\delta\chi_{c,\text{env}} \approx \frac{e^{N\gamma t/2}}{N\sqrt{Tt}}. \quad (24)$$

This can also be extrapolated from the analytical envelope for $N = 2$, Eq. (19). To this end, in Eq. (19) we introduce the substitutions $2\chi \rightarrow N\chi$ and $\gamma \rightarrow N\gamma/2$. If we now assume $\gamma/2N\chi^2 \ll 1$, Eq. (24) follows. This approximation does not take into account the small oscillations we observe for $\delta\chi_c$ around this envelope in Fig. 1(a). The minimum of Eq. (24)

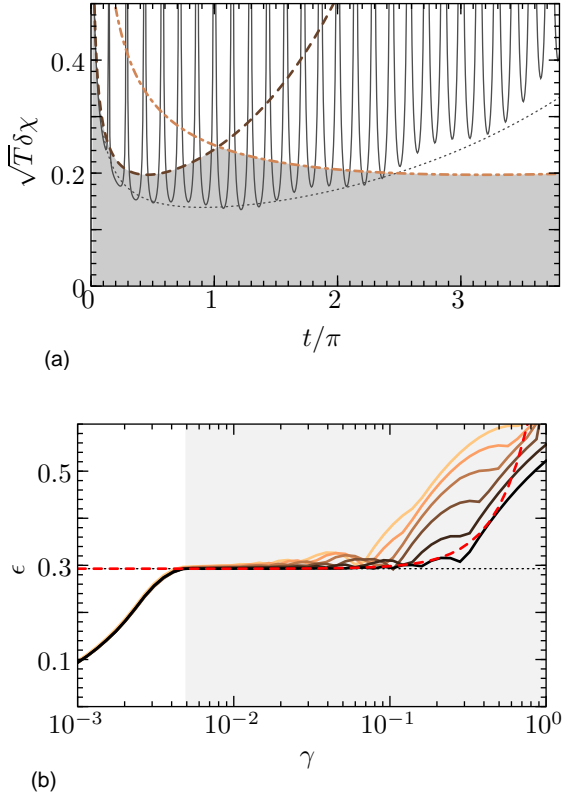


FIG. 1: (Color online) Cluster states vs reference system (I). Plot (a) shows the rescaled deviation for the cluster state setup (solid line), and the envelopes for maximally entangled states, Eq. (22) (dashed line), uncorrelated states, Eq. (23) (dashed-dotted line) in reference system (I), and cluster states, Eq. (24) (dotted line), all with $N = 7$. The shaded area is the area of possible improvement, which is penetrated by the cluster state scheme deviation. In (b) we plot the improvement of the cluster state scheme vs maximally entangled states in reference system (I) for $N = 2, 3, 4, 5, 6, 7$ (dark to light lines). Uncorrelated states lead to very similar curves. The dashed line indicates the analytical approximation, Eq. (21). The evolution time was kept constant for each N at $t_f(N) = \lceil 1/0.005N \rceil$ so we expect major improvements for $\gamma > 0.005$ in the shaded area. The horizontal dotted line marks the constant improvement $1 - 1/\sqrt{2}$. For all curves $\chi = 1$ and in (a) $\gamma = 0.05$.

and the time at which the minimum is attained are given by

$$\delta\chi_{c,\min} = \sqrt{\frac{\gamma e}{TN}}, \quad (25)$$

$$t_{c,\min} = \frac{1}{N\gamma}. \quad (26)$$

This indicates that, for $\gamma/\chi \ll 1$, we can expect the improvement, Eq. (20), of the minimal deviation to be $\epsilon \approx 1 - 1/\sqrt{2} \approx 29.3\%$ compared to more common schemes with maximally entangled and uncorrelated states. This is consistent with our result for $N = 2$, where we obtained the same improvement to lowest order in γ/χ . Indeed if we plot the improvement for varying γ for $N \geq 2$, we recover this behavior for small γ/χ

(onset of the light shaded area in Fig. 1(b)). For Fig. 1(b) we fixed the evolution time to $t = t_f(N)$. This means that from a finite $\gamma_f \propto 1/Nt_f(N)$ the minimum is expected to lie outside the integration domain, which leads to the observed deviation from the constant value in the white area ($\gamma < \gamma_f$) of the figure. For $N = 2$ we know that the improvement will deviate from the constant value $1 - 1/\sqrt{2}$ as $\gamma/\chi \rightarrow 1$.

We now focus on the substructure of kinks and humps of the $N = 2$ curve (black line) in Fig. 1(b). Analyzing the position of the local maxima (humps) allows us to determine the frequency $\Omega = \sqrt{4\chi^2 - \gamma^2}$. The humps are the result of the minimum of a lobe of the actual curve for $\delta\chi$ hitting the global minimum of the envelope of $\delta\chi_c$. This happens when the condition, Eq. (18), is satisfied at $t_{\min} = 1/N\gamma$. Hence for $N = 2$ we rewrite Eq. (18) as

$$\begin{aligned} \Omega t_{\min} &= \frac{\Omega}{2\gamma} \approx \frac{k\pi}{2} \\ \Rightarrow \gamma &= \frac{2\chi}{\sqrt{(k\pi)^2 + 1}} \sim \frac{\chi}{k\pi/2} \quad (k \text{ odd}). \end{aligned}$$

For the parameters in Fig. 1(b) the zeroth-order approximation we used in this calculation locates the humps reasonably accurate for $k \geq 3$. For $k = 1$ one would have to take into account higher-order terms in γ/Ω (cf. Eq. (18)). In between the humps for different k the kinks indicate where the lobe of $\delta\chi$ closest to the global minimum of the envelope is least optimal. We observe that qualitatively the same substructure persists for higher N but the humps slightly shift position and larger improvement sets in at lower γ .

IV. DEPOLARIZATION AND PURE DAMPING

In this section, we focus on two further noise channels, namely, depolarization and pure damping with the corresponding master equations

$$\begin{aligned} \frac{d\rho}{dt}(t) &= i[\rho, H_\chi] + \frac{\gamma}{4} \sum_{j=1}^N \left(2\sigma_-^{(j)} \rho \sigma_+^{(j)} - \sigma_+^{(j)} \sigma_-^{(j)} \rho - \rho \sigma_+^{(j)} \sigma_-^{(j)} \right. \\ &\quad \left. + 2\sigma_+^{(j)} \rho \sigma_-^{(j)} - \sigma_-^{(j)} \sigma_+^{(j)} \rho - \rho \sigma_-^{(j)} \sigma_+^{(j)} \right. \\ &\quad \left. + \sigma_z^{(j)} \rho \sigma_z^{(j)} - \rho \right), \end{aligned} \quad (27)$$

$$\begin{aligned} \frac{d\rho}{dt}(t) &= i[\rho, H_\chi] \\ &\quad + \frac{\gamma}{2} \sum_{j=1}^N \left(2\sigma_+^{(j)} \rho \sigma_-^{(j)} - \sigma_-^{(j)} \sigma_+^{(j)} \rho - \rho \sigma_-^{(j)} \sigma_+^{(j)} \right), \end{aligned} \quad (28)$$

respectively [35, 39]. Here we used $\sigma_\pm := (1/2)(\sigma_x \pm i\sigma_y)$. In this section, we use system (I) as reference. Depolarization occurs when the system interacts with a bath in the high-temperature limit $T \rightarrow \infty$. This drives the qubits into a completely depolarized state, i.e., $\lim_{t \rightarrow \infty} \langle \sigma_z \rangle = 0$. Pure damping, on the other hand, describes the decay of every qubit

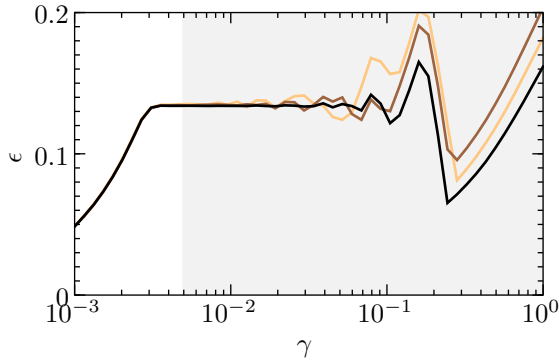


FIG. 2: (Color online) Improvement of cluster states vs maximally entangled states in reference system (I) under depolarization. In this plot $N = 2, 4, 6$ (dark to light lines) and $\chi = 1$. For uncorrelated states we get qualitatively similar results because both attain the same minimum. The shaded area indicates the region beyond the cutoff $\gamma_f = 0.005$.

into the state $|0\rangle$. Under the depolarizing channel, Eq. (27), both maximally entangled and uncorrelated states yield the same deviation as with dephasing (assuming the same measurements M_u and M_c , respectively). This is the result of their measurements only extracting the “transversal” evolution depending on σ_x , whereas the depolarizing channel changes decoherence in the longitudinal direction. On the other hand, the damping channel, Eq. (28), has the transversal effect of reducing the decay rate by one-half for maximally entangled and uncorrelated states [35]. Hence for the polarizing channel we can use envelopes, Eqs. (22) and (23), and for the damping channel we replace γ by $\gamma/2$ in these envelopes. This leads to the minima

$$\begin{aligned} \delta\chi_{m,env} &= \sqrt{\frac{\gamma e}{TN}} & \text{at } t_{m,min} &= \frac{1}{N\gamma}, \\ \delta\chi_{u,min} &= \sqrt{\frac{\gamma e}{TN}} & \text{at } t_{u,min} &= \frac{1}{\gamma}. \end{aligned}$$

Both minima are the same and their value is, in fact, the same minimum we approximated for cluster states in the dephasing channel in the preceding section. However, a priori it is unclear how the cluster states will evolve under these different master equations.

First we discuss numerical results for the depolarizing channel. In Fig. 2 we plot the improvement of cluster states vs maximally entangled states in reference system (I). Similar to dephasing noise the improvement saturates for intermediate γ before it starts to oscillate as the noise γ approaches the strength of the parameter χ . The constant improvement in the depolarization case is lower than for dephasing at $\epsilon \approx 13\%$. We observe a very similar behavior if we take uncorrelated states as reference because their deviation attains the same minimum under depolarization as maximally entangled states. As expected, the improvement decreases for γ below the cutoff γ_f , which defines a maximal evolution time as before.

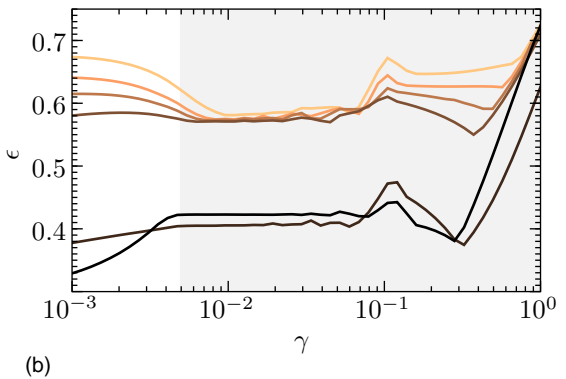
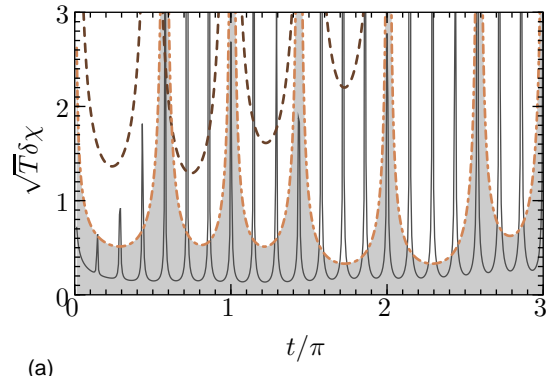


FIG. 3: (Color online) Cluster state vs reference system (II) under dephasing noise. (a) shows the rescaled deviations and (b) the relative improvement with uncorrelated states. The same parameters and notation as in Fig. 1 apply but here we expose maximally entangled and uncorrelated states to reference system (II). In contrast to Fig. 1, we do not plot envelopes in (a) but the actual deviation for the given parameters.

For the damping channel we could not observe a global improvement of the cluster state setup compared to either maximally entangled or uncorrelated states in reference system (I). The deviation for cluster states is nearly identical to the one for maximally entangled states. This is caused by the reduced decoherence rate of both reference states under damping as mentioned above. Hence, in a system which is purely subject to damping, cluster states offer no improvement in terms of minimal deviation over preparing a system in reference (I). However, experiments are often prone to a combination of errors and all other noise models we studied offered an overall improvement.

V. RESULTS FOR REFERENCE SYSTEM (II)

In this section, we discuss all three noise models but now compare the cluster state setup with reference system (II). We start with the results for dephasing noise. In Fig. 3(a) we plot the deviations for maximally entangled states (dashed lines) and uncorrelated states (dashed-dotted) and compare it to $\delta\chi_c$

of the cluster states (solid). We do not use the envelope as before because we did not derive an analytical solution for the reference states in system (II). Instead the curves represent the actual numerical deviations for a specific set of parameters. Similarly to reference system (I), cluster states attain the lowest overall deviation. Maximally entangled states prove useless in this setup as their deviation is almost one order of magnitude larger than for cluster states or even uncorrelated states. Their frequency also does not depend on N , which is the fact that causes their advantage in the noise-free case of setup (I). The curve for uncorrelated states exhibits a “bimodal” structure, where the lobes follow two sets of envelopes with different dephasing rates. If we plot the improvement ϵ in Fig. 3(b), it becomes apparent that the enhancement achievable with cluster states is even more pronounced than in reference system (I). The nature of the sharp divide between the improvements for $N = 2, 3$ and higher N is unclear. The reason for the larger improvement for $\gamma < \gamma_f = 0.005$ in some curves is that the deviation of the uncorrelated states reaches its minimum after the cluster states. In this regime of γ the reference system has not yet reached its minimum at the cutoff time t_f , whereas the cluster state deviation is closer to its minimum or has already reached it. Similar to the results with reference system (I), we find plateaus for small γ , which indicate that we have again a constant offset as γ approaches 0. For the resource sizes considered in the plot, these constant values correspond to improvements of approximately 40% and 60%.

In contrast to the case with system (I), when we let the reference states evolve under the depolarizing and pure damping master equations, we do observe a notable deviation improvement with cluster states under these noise models. The results for damping in Figs. 4(a,b) suggest a steady increase of the improvement for higher particle numbers. One curiosity is the result for the $N = 2$ maximally entangled state in Fig. 4(b) (black curve). In this case, the expectation value of M_m does not exhibit oscillations in time, which makes this state unsuitable for the parameter estimation. For higher N we do recover oscillations but still see a large advantage of cluster states. The results for depolarization are similar with similar magnitudes of improvement for both reference states.

VI. SCALING

We have seen in Sec. II that, in principle, our scheme can achieve the Heisenberg limit in the number of qubits N for decoherence-free systems. For dephasing noise we have given an approximation of the envelope of the deviation Eq. (24), which results in a shot-noise-limited scaling, Eq. (25). In this section, we consider experiments with a fixed evolution time and derive the scaling properties of the deviation in this limit.

We consider γt to be a small parameter. Then we can expand Eq. (24) to first order

$$\delta\chi_{c,\text{env}} = \frac{1}{N\sqrt{Tt}} + \frac{\gamma}{2}\sqrt{\frac{t}{T}} + \mathcal{O}\left((N\gamma t/2)^2\right). \quad (29)$$

The first term on the right-hand side is a Heisenberg scaling with $1/N$ and the second term is a constant offset of the devi-

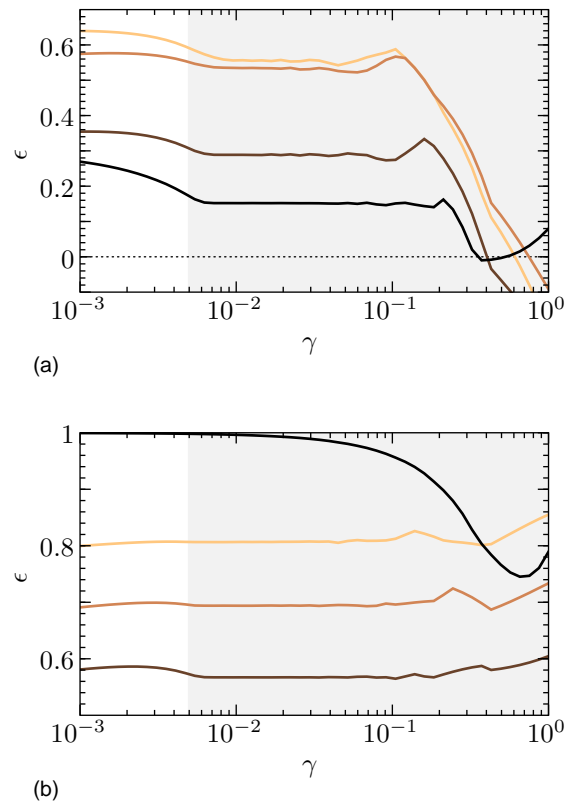


FIG. 4: (Color online) Improvement of cluster states vs (a) uncorrelated states and (b) maximally entangled states in reference system (II) under damping. Both plots show $N = 2, 3, 4, 6$ (from dark to light) with $\chi = 1$ and $\gamma_f = 0.005$ (marked by the shaded area).

ation. We compare this expansion with the expansions of the deviation of maximally entangled and uncorrelated states in reference system (I), Eqs. (22) and (23),

$$\delta\chi_{m,\text{env}} = \frac{1}{N\sqrt{Tt}} + \gamma\sqrt{\frac{t}{T}} + \mathcal{O}\left[(N\gamma t)^2\right], \quad (30)$$

$$\delta\chi_{u,\text{env}} = \frac{1}{\sqrt{NTt}} + \frac{\gamma\sqrt{t}}{\sqrt{NT}} + \mathcal{O}\left[(\gamma t)^2\right]. \quad (31)$$

First we note that the constant offset (second term on the right-hand side) for cluster states in Eq. (29) is only one-half the offset for maximally entangled states in Eq. (30), and also smaller than the second term in Eq. (31). This guarantees that in this limit the deviation of the cluster states is always smaller than in both reference systems. Furthermore, the approximation for cluster states is valid for $(N\gamma t/2)^2 \ll 1$, whereas for maximally entangled states it is only valid for $(N\gamma t)^2 \ll 1$. For fixed γt we can thus expect the deviation of the cluster states to scale with the Heisenberg limit (first term in the expansion) for 2 times as many qubits as with maximally entangled states. In the limit considered here, uncorrelated states only scale with the shot-noise limit. For small numbers of qubits and small fixed γt the cluster state setup is superior in scaling to both reference schemes.

VII. CONCLUSION

We have introduced cluster states into parameter estimation theory. By using “maximally entangled” cluster states as a probe in a system evolving under a three-body Hamiltonian, we could show that it is possible to achieve the Heisenberg limit of sensitivity to the parameter. The addition of dephasing noise leads to decoherence in the system but our results indicate that the decoherence rate is reduced compared to the standard setup in quantum parameter estimation with maximally entangled states. This leads to an improvement of the minimally achievable deviation. This improvement also persists when the cluster state setup is compared to different reference setups. The results suggest that the improvement for a given number of qubits is almost constant when the strength of the noise is much smaller than the parameter, which is often desirable in experiments. Similar results hold when the qubits are subject to depolarization or damping noises.

The creation of 1D cluster states in optical lattices typically results in cluster sizes on the order of $N \approx 40$ [10]. Also proposals for implementing three-body Hamiltonians have been devised for optical lattices [17, 18], which makes this system an ideal candidate for our measurement scheme. The achievable number of qubits could be increased even further by extending the present scheme to higher-dimensional cluster states. These can be created in optical lattices by using state-dependent lattice shifts.

Analogous to parameter estimation with maximally entangled states, the Heisenberg scaling does not persist for large systems under decoherence. However, for small systems we have shown that the deviation of the cluster state setup scales at the Heisenberg limit. In the cluster state setup, this limit can be realized for 2 times as many qubits as with maximally entangled or uncorrelated states.

Acknowledgments

This research was supported by the European Commission under the Marie Curie Programme through QIPEST.

APPENDIX: ANALYTICAL SOLUTION OF THE DEPHASING MASTER EQUATION FOR $N = 2$

To illustrate the behavior of the deviation $\delta\chi_c$, we derive an analytical solution of the master equation (14) with the clus-

ter Hamiltonian Eq. (6) for the case $N = 2$. Finding a solution for higher N is complicated by the fact that the basis of the underlying Hilbert space grows exponentially with N . In the following derivation we use the convention $\sigma_0 := I$, $\sigma_{1,2,3} := \sigma_{x,y,z}$, where I is the identity. With this notation the full Hamiltonian is given by

$$H_{II} = \frac{\chi}{2} \left(K^{(1)} + K^{(2)} \right) = \frac{\chi}{2} \left(\sigma_1^{(1)} \sigma_3^{(2)} + \sigma_3^{(1)} \sigma_1^{(2)} \right).$$

The master equation takes the form

$$\begin{aligned} \frac{d\rho}{dt}(t) = & i \frac{\chi}{2} \left\{ \left[\rho(t), K^{(1)} \right] + \left[\rho(t), K^{(2)} \right] \right\} \\ & + \frac{\gamma}{2} \left[\sigma_3^{(1)} \rho(t) \sigma_3^{(1)} + \sigma_3^{(2)} \rho(t) \sigma_3^{(2)} - 2\rho(t) \right]. \end{aligned} \quad (\text{A.1})$$

We expand $\rho(t) \in L(\mathcal{H}^{\otimes 2})$ in the Pauli basis for two qubits

$$\rho(t) = \sum_{i,j=0}^3 c_{ij}(t) \sigma_i \otimes \sigma_j,$$

where $c_{ij}(t)$ are the time-dependent coefficients of the corresponding basis vectors in $L(\mathcal{H}^{\otimes 2})$. For $\rho(t)$ to be of unit trace we must have $c_{00}(t) = 1/2^N = 1/4$. For the commutators in Eq. (A.1) we only need to consider terms in the expansion of $\rho(t)$ where both Pauli matrices in the direct product do not commute with $\sigma_1 \otimes \sigma_3$ and $\sigma_3 \otimes \sigma_1$. For the commutator with $K^{(1)}$ ($K^{(2)}$) the commuting vectors are $\sigma_0 \otimes \sigma_0$, $\sigma_0 \otimes \sigma_3$, $\sigma_1 \otimes \sigma_0$, and $\sigma_1 \otimes \sigma_3$ ($\sigma_0 \otimes \sigma_0$, $\sigma_0 \otimes \sigma_1$, $\sigma_3 \otimes \sigma_0$, and $\sigma_3 \otimes \sigma_1$). Each commutator is then a linear combination in the subspace orthogonal to the one spanned by the four commuting vectors. The incoherent part of the master equation can be easily evaluated by noting that $\sigma_3^{(i)} \rho(t) \sigma_3^{(i)}$ flips the signs of the components which contain $\sigma_1^{(i)}$ or $\sigma_2^{(i)}$. These observations allow us to rewrite the master equation as a system of coupled ODEs in the coefficients, which we write as a vector $c(t) = [c_{01}(t), c_{02}(t), \dots]$. Note that the component $c_{00}(t)$ is constant which does not affect the other coefficients so we do not include it in this calculation. In terms of this vector the system of ODEs becomes

$$\frac{dc}{dt}(t) = Ac(t). \quad (\text{A.2})$$

By evaluating the commutators and the incoherent part of the master equation we find for the matrix A ,

$$A = \begin{pmatrix} -\gamma & 0 & 0 & 0 & 0 & -\chi & 0 & 0 & 0 & 0 & 0 & 0 & 0 & 0 & 0 \\ 0 & -\gamma & 0 & 0 & \chi & 0 & 0 & 0 & 0 & 0 & 0 & 0 & 0 & 0 & -\chi \\ 0 & 0 & 0 & 0 & 0 & 0 & 0 & 0 & 0 & 0 & 0 & 0 & 0 & \chi & 0 \\ 0 & 0 & 0 & -\gamma & 0 & 0 & 0 & 0 & -\chi & 0 & 0 & 0 & 0 & 0 & 0 \\ 0 & -\chi & 0 & 0 & -2\gamma & 0 & 0 & -\chi & 0 & 0 & 0 & 0 & 0 & 0 & 0 \\ \chi & 0 & 0 & 0 & 0 & -2\gamma & 0 & 0 & 0 & 0 & i\chi & 0 & 0 & 0 & 0 \\ 0 & 0 & 0 & 0 & 0 & 0 & -\gamma & 0 & 0 & -i\chi & 0 & 0 & 0 & 0 & 0 \\ 0 & 0 & 0 & 0 & \chi & 0 & 0 & -\gamma & 0 & 0 & 0 & 0 & 0 & 0 & -\chi \\ 0 & 0 & 0 & \chi & 0 & 0 & 0 & 0 & -2\gamma & 0 & 0 & 0 & 0 & 0 & i\chi \\ 0 & 0 & 0 & 0 & 0 & 0 & -i\chi & 0 & 0 & -2\gamma & 0 & 0 & -i\chi & 0 & 0 \\ 0 & 0 & 0 & 0 & 0 & i\chi & 0 & 0 & 0 & 0 & -\gamma & -\chi & 0 & 0 & 0 \\ 0 & 0 & 0 & 0 & 0 & 0 & 0 & 0 & 0 & 0 & \chi & 0 & 0 & 0 & 0 \\ 0 & 0 & 0 & 0 & 0 & 0 & 0 & 0 & 0 & -i\chi & 0 & 0 & -\gamma & 0 & 0 \\ 0 & 0 & -\chi & 0 & 0 & 0 & 0 & 0 & i\chi & 0 & 0 & 0 & 0 & -\gamma & 0 \\ 0 & \chi & 0 & 0 & 0 & 0 & 0 & \chi & 0 & 0 & 0 & 0 & 0 & 0 & 0 \end{pmatrix}.$$

This matrix is not time dependent so the solution of the ODE (A.2) is

$$c(t) = e^{At}c(0),$$

where $c(0)$ are the components of the initial state. For the 1D cluster state with $N = 2$ the initial values are given by

$$c_{00}(0) = \frac{1}{4}, \quad c_{11}(0) = -\frac{1}{4}, \quad c_{22}(0) = \frac{1}{4}, \quad c_{33}(0) = \frac{1}{4}$$

and all other components vanish. We only need to determine the quantity of interest $\langle M_c \rangle_t = \text{tr}[M_c \rho(t)]$, which can be derived from the solution $c(t)$. The measurement operator $M_c = \sigma_3 \otimes \sigma_3$ leaves only one component of $\rho(t)$ with nonzero trace

$$\begin{aligned} \langle M_c \rangle_t &= \text{tr}[c_{33}(t)\sigma_0 \otimes \sigma_0] = 4c_{33}(t) \\ &= e^{-\gamma t} \left(\cos(\Omega t) + \frac{\gamma}{\Omega} \sin(\Omega t) \right), \end{aligned}$$

where $\Omega = \sqrt{4\chi^2 - \gamma^2}$. This leaves us with the solution for the deviation

$$\begin{aligned} \delta\chi_c(t) &= \frac{\Delta M_c}{\sqrt{T/t} |d\langle M_c \rangle_t / d\chi|} \\ &= \frac{e^{\gamma t} \sqrt{1 - e^{-2\gamma t} \left(\cos(\Omega t) + \frac{\gamma}{\Omega} \sin(\Omega t) \right)^2}}{\sqrt{Tt} \frac{4\chi}{\Omega} \left| \frac{\gamma}{\Omega} \cos(\Omega t) - \left(1 + \frac{\gamma}{\Omega^2 t} \right) \sin(\Omega t) \right|}. \end{aligned}$$

We note that for $\gamma/\Omega \rightarrow 0$ this deviation approaches the deviation for maximally entangled states with Hamiltonian H_I and a decoherence rate reduced by half [cf. Eq. (17)].

In a similar way one derives the solution for $N = 1$, which is given by

$$\delta\chi_c(t) = \frac{e^{\gamma t/2} \sqrt{1 - e^{-\gamma t} \left(\cos(\Omega t/2) + \frac{\gamma}{\Omega} \sin(\Omega t/2) \right)^2}}{\sqrt{Tt} \frac{2\chi}{\Omega} \left| \frac{\gamma}{\Omega} \cos(\Omega t/2) - \left(1 + \frac{2\gamma}{\Omega^2 t} \right) \sin(\Omega t/2) \right|}.$$

Comparing this form with $\delta\chi_c(t)$ suggests an obvious extension to $N > 2$ by replacing the dephasing rate with $N\gamma/2$ and the frequencies by $N\Omega/2$ in $\langle M_c \rangle_t$. However, we could not verify numerically that this generalized solution holds for $N > 2$. The numerical solutions for $N > 2$ follow this extrapolation closely but not exactly [cf. Fig. 1(a)].

-
- [1] J. J. Bollinger, W. M. Itano, D. J. Wineland, and D. J. Heinzen, Phys. Rev. A **54**, R4649 (1996).
- [2] V. Giovannetti, S. Lloyd, and L. Maccone, Nature **412**, 417 (2001).
- [3] K. Nemoto, W. J. Munro, G. J. Milburn, and S. L. Braunstein, in *Proceedings of the Sixth International Conference on Quantum Communication, Measurement and Computing*, edited by J. H. Shapiro and O. Hirota (Rinton Press, Princeton, NJ, 2003), p. 333, [arXiv:quant-ph/0312063](#).
- [4] S. Lloyd, Science **321**, 1463 (2008), [arXiv:0803.2022](#).
- [5] V. Giovannetti, S. Lloyd, L. Maccone, and J. H. Shapiro, Phys. Rev. A **79**, 013827 (2009), [arXiv:0804.2875](#).
- [6] S. F. Huelga, C. Macchiavello, T. Pellizzari, A. K. Ekert, M. B. Plenio, and J. I. Cirac, Phys. Rev. Lett. **79**, 3865 (1997), [arXiv:quant-ph/9707014](#).
- [7] R. Raussendorf and H. J. Briegel, Phys. Rev. Lett. **86**, 5188 (2001).
- [8] H. J. Briegel and R. Raussendorf, Phys. Rev. Lett. **86**, 910 (2001), [arXiv:quant-ph/0004051](#).
- [9] W. Dür and H.-J. Briegel, Phys. Rev. Lett. **92**, 180403 (2004),

- [arXiv:quant-ph/0307180](https://arxiv.org/abs/quant-ph/0307180).
- [10] O. Mandel, M. Greiner, A. Widera, T. Rom, T. W. Hänsch, and I. Bloch, *Nature* **425**, 937 (2003).
- [11] P. A. Ivanov, N. V. Vitanov, and M. B. Plenio, *Phys. Rev. A* **78**, 012323 (2008).
- [12] X. B. Zou and W. Mathis, *Phys. Rev. A* **72**, 013809 (2005).
- [13] J. Cho and H.-W. Lee, *Phys. Rev. Lett.* **95**, 160501 (2005).
- [14] T. Tanamoto, Y. X. Liu, S. Fujita, X. Hu, and F. Nori, *Phys. Rev. Lett.* **97**, 230501 (2006).
- [15] S. R. Clark, C. Moura Alves, and D. Jaksch, *New J. Phys.* **7**, 124 (2005).
- [16] S. R. Clark, A. Klein, M. Bruderer, and D. Jaksch, *New J. Phys.* **9**, 202 (2007), [arXiv:0705.3584](https://arxiv.org/abs/0705.3584).
- [17] H. P. Büchler, A. Micheli, and P. Zoller, *Nat. Phys.* **3**, 726 (2007), [arXiv:cond-mat/0703688](https://arxiv.org/abs/cond-mat/0703688).
- [18] J. K. Pachos and M. B. Plenio, *Phys. Rev. Lett.* **93**, 056402 (2004), [arXiv:quant-ph/0401106](https://arxiv.org/abs/quant-ph/0401106).
- [19] S. Boixo, A. Datta, S. T. Flammia, A. Shaji, E. Bagan, and C. M. Caves, *Phys. Rev. A* **77**, 012317 (2008), [arXiv:0710.0285](https://arxiv.org/abs/0710.0285).
- [20] S. Boixo, S. T. Flammia, C. M. Caves, and J. M. Geremia, *Phys. Rev. Lett.* **98**, 090401 (2007), [arXiv:quant-ph/0609179](https://arxiv.org/abs/quant-ph/0609179).
- [21] S. Choi and B. Sundaram, *Phys. Rev. A* **77**, 053613 (2008), [arXiv:0709.3842](https://arxiv.org/abs/0709.3842).
- [22] P. Walther, K. J. Resch, T. Rudolph, E. Schenck, H. Weinfurter, V. Vedral, M. Aspelmeyer, and A. Zeilinger, *Nature* **434**, 169 (2005), [arXiv:quant-ph/0503126](https://arxiv.org/abs/quant-ph/0503126).
- [23] N. Kiesel, C. Schmid, U. Weber, G. Tóth, O. Gühne, R. Ursin, and H. Weinfurter, *Phys. Rev. Lett.* **95**, 210502 (2005).
- [24] A.-N. Zhang, C.-Y. Lu, X.-Q. Zhou, Y.-A. Chen, Z. Zhao, T. Yang, and J.-W. Pan, *Phys. Rev. A* **73**, 022330 (2006).
- [25] C.-Y. Lu, X.-Q. Zhou, O. Gühne, W.-B. Gao, J. Zhang, Z.-S. Yuan, A. Goebel, T. Yang, and J.-W. Pan, *Nat. Phys.* **3**, 91 (2007).
- [26] G. Vallone, E. Pomarico, P. Mataloni, F. De Martini, and V. Berardi, *Phys. Rev. Lett.* **98**, 180502 (2007), [arXiv:quant-ph/0703191](https://arxiv.org/abs/quant-ph/0703191).
- [27] U. Dorner, R. Demkowicz-Dobrzanski, B. J. Smith, J. S. Lundeen, W. Wasilewski, K. Banaszek, and I. A. Walmsley, *Phys. Rev. Lett.* **102**, 040403 (2009), [arXiv:0807.3659](https://arxiv.org/abs/0807.3659).
- [28] S. L. Braunstein and C. M. Caves, *Phys. Rev. Lett.* **72**, 3439 (1994).
- [29] V. Giovannetti, S. Lloyd, and L. Maccone, *Phys. Rev. Lett.* **96**, 010401 (2006), [arXiv:quant-ph/0509179](https://arxiv.org/abs/quant-ph/0509179).
- [30] S. L. Braunstein, C. M. Caves, and G. J. Milburn, *Ann. Phys.* **247**, 135 (1996), [arXiv:quant-ph/9507004](https://arxiv.org/abs/quant-ph/9507004).
- [31] D. Ulam-Orgikh and M. Kitagawa, *Phys. Rev. A* **64**, 052106 (2001).
- [32] A. Shaji and C. M. Caves, *Phys. Rev. A* **76**, 032111 (2007), [arXiv:0705.1002](https://arxiv.org/abs/0705.1002).
- [33] M. Hein, J. Eisert, and H. J. Briegel, *Phys. Rev. A* **69**, 062311 (2004), [arXiv:quant-ph/0307130](https://arxiv.org/abs/quant-ph/0307130).
- [34] F. Harary, *Graph Theory* (Addison-Wesley, Reading, MA, 1969).
- [35] M. Hein, W. Dür, and H.-J. Briegel, *Phys. Rev. A* **71**, 032350 (2005), [arXiv:quant-ph/0408165](https://arxiv.org/abs/quant-ph/0408165).
- [36] C. Simon and J. Kempe, *Phys. Rev. A* **65**, 052327 (2002), [arXiv:quant-ph/0109102](https://arxiv.org/abs/quant-ph/0109102).
- [37] M. Hein, W. Dür, J. Eisert, R. Raussendorf, M. van den Nest, and H. J. Briegel, in *Proceedings of the International School of Physics Enrico Fermi on Quantum Computers, Algorithms and Chaos*, edited by P. Z. G. Casati, D. L. Shepelyansky and G. Benenti (IOS Press, Varenna, Italy, 2005), [arXiv:quant-ph/0602096](https://arxiv.org/abs/quant-ph/0602096).
- [38] G. A. Durkin and J. P. Dowling, *Phys. Rev. Lett.* **99**, 070801 (2007), [arXiv:quant-ph/0607088](https://arxiv.org/abs/quant-ph/0607088).
- [39] H.-J. Briegel and B.-G. Englert, *Phys. Rev. A* **47**, 3311 (1993).